

Testing a drone motor with single point vibrometry

SmarAct GmbH

1. INTRODUCTION

Vibrations play a critical role in the performance of flying machines such as drones. Material fatigue and the loosening of parts are the most pronounced consequences of vibrations. More subtle effects are poor maneuverability due to vibrating gyroscopes and the reduced quality of video recordings. As a first step towards minimizing such effects, the vibrations need to be quantified. In this application note, we demonstrate the use of SmarAct's **PICOSCALE** Interferometer for the contactless measurement of vibrations generated by a rotor of a commercial drone.

2. METHODS

The experiments were performed with a standard **PICOSCALE** Interferometer. The motor was removed from the drone and mounted on an aluminium plate. In order to obtain an idea about the transmission of vibrations, two sensor heads, one line focusing head, and one with a collimated laser beam, were used. The line focusing head S_2 was aimed directly at the rotating rotor shaft while the other, S_1 , was aimed at the stationary base of the motor, as shown on Figure 1. A strip of retro-reflective tape was placed on the base to simplify adjustment. The rotor itself was polished. The motor speed was set to approximately 21000 rpm (350 Hz), a common speed for drones. The displacement signals were sampled at 156.25 kHz for 1 s. In a second step, the speed of the rotor was slowly decreased over 5 s to further dissect the spectrum of vibrations.

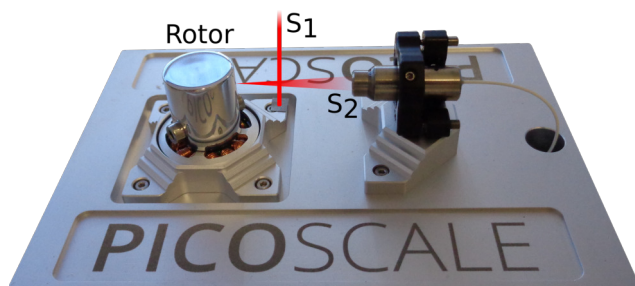


Figure 1. Experimental setup to measure the vibrations induced by the rotor of a drone. Two sensor heads were used: S_1 , a collimated sensor head (not shown) pointing towards the base, and S_2 a line focusing sensor head aiming at the rotor.

3. RESULTS

The measured displacement signals are shown in Figure 2. The vibration amplitude measured at the base is about two orders of magnitude lower than at the rotor itself: the peak-to-peak amplitude on the rotor is roughly $150\ \mu\text{m}$ but only $1\ \mu\text{m}$ at the base. This indicates that within the motor already a large damping of the vibrations takes place. It should be noted that inhomogeneities on the surface of a non-perfectly cylindrical rotor can also induce "spikes" oscillating either at the rotor frequency or at its harmonics. This is due to the fact that these inhomogeneities will be seen as displacement changes, thus measured. However, here, their effects do not appear to dominate the vibration measurements as both spectra display similar peaks distribution. Thus, for the sake of simplicity, geometrical artifacts are not taken into consideration and neglected within this study.

Identifying vibrations from time series only can be difficult and it is usually preferred to apply a Fourier transformation to the data so that the various vibration components can be investigated in the frequency domain. Here, each frequency component will be visible as a peak in the spectrum, where the peak height directly depends on the vibration amplitude. This spectral dissection allows a much clearer analysis of the generated vibrations.

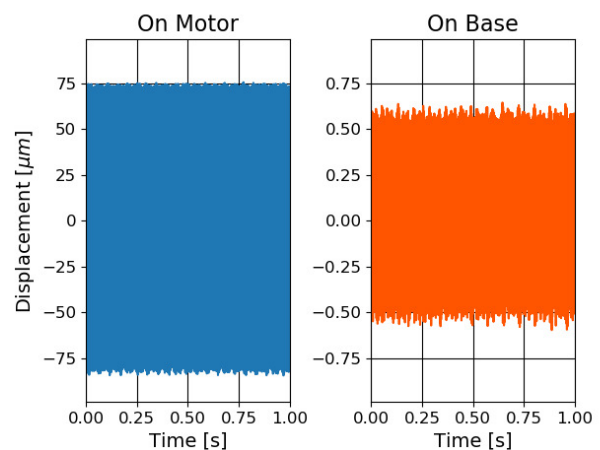


Figure 2. 1 s displacement signals measured on the motor and on the base when the rotor moves at 350 Hz. The oscillation amplitude is almost 100 times lower on the base than on the rotor itself.

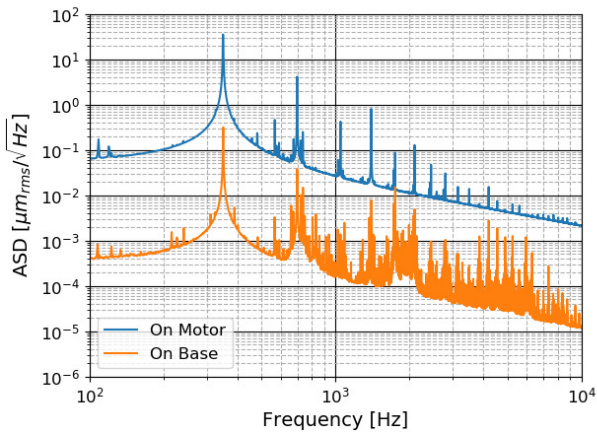


Figure 3. Amplitude Spectral Densities (ASD) of 100 time series on the rotor and on the base. The vibrations transduced into the base are two orders of magnitude lower than on the rotor itself which indicates the presence of a significant damping.

To obtain a high signal-to-noise ratio, 100 time series were recorded and their corresponding Fourier spectra averaged (Figure 3).

A pronounced peak at the rotor speed of 350 Hz and peaks at its harmonics (at 700, 1150, 1400, .. Hz) are visible in both the rotor and the base spectra. Interestingly, the active rotor induces a plethora of additional peaks as well, more visible in the spectrum of the base, which are likely caused by other components that are set into resonance by the spinning rotor.

To identify such peaks, a spectrogram can be reconstructed after recording a long time series while reducing the motor frequency. Peaks induced by the rotor will reveal themselves because they will follow the reduction frequency. Peaks that show resonances of other components will not change frequency when the rotor speed is reduced, although their amplitude may change.

Figure 4 shows the corresponding spectrogram recorded while the motor frequency was reduced in the course of 5 s. The fundamental rotor frequency, shown by the red line *a*, and its harmonics can be clearly seen to reduce from $t = 0.6$ s. Some resonance remain however undisturbed as in region *b*, and thus originate from other parts in or near the motor. Finally, there is a pronounced resonance present in the system at 2.6 s, region *c*. This gets excited during the slowing down of the rotor because one of the stronger higher harmonics reaches 1.575 kHz. At this time, components from the system appear to resonate, yet with low intensity as the magnitude does not exceed 35 dB, approximately $1 \mu\text{m}$. This multi-resonance state quickly vanishes however as the deceleration of the rotor continues.

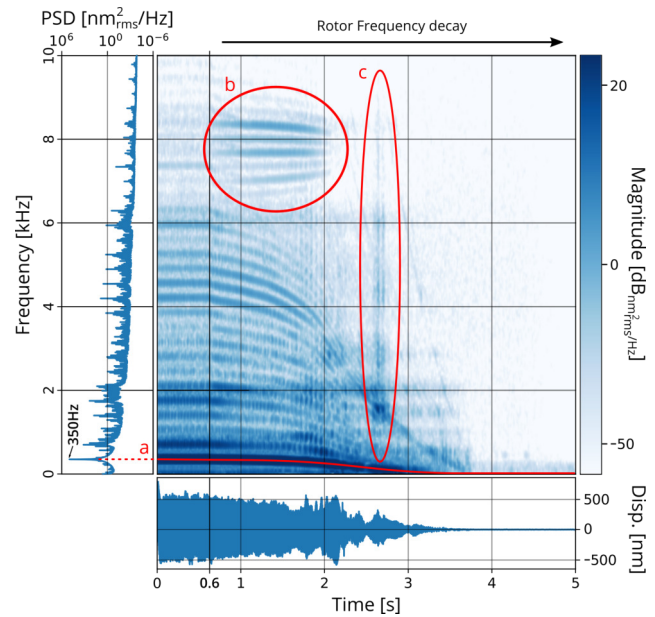


Figure 4. Reconstructed spectrogram after recording a 5 s displacement (Disp.) signal, shown at the bottom. The spectrogram magnitude in $\text{dB}_{\text{n.m}^2/\text{Hz}}$ is referenced to $1 \text{ nm}^2/\text{Hz}$. The active rotor induces large vibrations, as seen in the Power Spectral Density (PSD) on the left.

4. CONCLUSION

The PICOSCALE Interferometer can be employed to investigate vibrations up to 2.5 MHz. Because up to 3 sensor heads can be used in parallel, vibrations can be measured at multiple points which can for example be useful to establish transfer functions. The picometer resolution and a sub-picometer noise floor means that even the smallest vibrations can be detected. Further options to focus the measurement spot or to scan the measurement beam for a full modal analysis are available.

Sales partner / Contacts

Germany

SmarAct GmbH

Schuette-Lanz-Strasse 9
26135 Oldenburg
Germany

T: +49 441 - 800 879 0
Email: info-de@smaract.com
www.smaract.com

France

SmarAct GmbH

Schuette-Lanz-Strasse 9
26135 Oldenburg
Germany

T: +49 441 - 800 879 956
Email: info-fr@smaract.com
www.smaract.com

USA

SmarAct Inc.

2140 Shattuck Ave. Suite 302
Berkeley, CA 94704
United States of America

T: +1 415 - 766 9006
Email: info-us@smaract.com
www.smaract.com

China

Dynasense Photonics

6 Taiping Street
Xi Cheng District,
Beijing, China

T: +86 10 - 835 038 53
Email: info@dyna-sense.com
www.dyna-sense.com

Natsu Precision Tech

Room 515, Floor 5, Building 7,
No.18 East Qinghe Anning
Zhuang Road,
Haidian District
Beijing, China

T: +86 18 - 616 715 058
Email: chenye@nano-stage.com
www.nano-stage.com

Shanghai Kingway Optech Co.Ltd

Room 1212, T1 Building
Zhonggeng Global Creative Center
Lane 166, Yuhong Road
Minhang District
Shanghai, China

Tel: +86 21 - 548 469 66
Email: sales@kingway-optech.com
www.kingway-optech.com

Japan

Physix Technology Inc.

Ichikawa-Business-Plaza
4-2-5 Minami-yawata,
Ichikawa-shi
272-0023 Chiba
Japan

T/F: +81 47 - 370 86 00
Email: info-jp@smaract.com
www.physix-tech.com

South Korea

SEUM Tronics

1109, 1, Gasan digital 1-ro
Geumcheon-gu
Seoul, 08594,
Korea

T: +82 2 - 868 10 02
Email: info-kr@smaract.com
www.seumtronics.com

Israel

Trico Israel Ltd.

P.O.Box 6172
46150 Herzeliya
Israel

T: +972 9 - 950 60 74
Email: info-il@smaract.com
www.trico.co.il